Minicourse in University of Auckland: Computational modeling of time-harmonic wave propagation

Teemu Luostari[1],
in collaboration with
Tomi Huttunen[1], Jari P. Kaipio[1,3], Peter Monk[2]

[1]Department of Physics and Mathematics, University of Eastern Finland, Finland
[2]Department of Mathematical Sciences, University of Delaware, USA
[3] Department of Mathematics, University of Auckland, New Zealand

6th September 2010

Wave equation can be written as

$$\nabla \cdot \left(\frac{1}{\rho} \nabla P(r,t) \right) - \frac{1}{\rho c^2} \frac{\partial^2 P(r,t)}{\partial t^2} = 0, \tag{1}$$

where $P(r,t)$ is pressure, ρ is the density and c is the speed of sound.
If pressure $P(r,t)$ is time-harmonic, i.e. $P(r,t) = p(r)\exp(-i\omega t)$ where the angular frequency $\omega = 2\pi f$ and t is the time, the time-harmonic (Helmholtz) equation is of the form

$$\nabla \cdot \left(\frac{1}{\rho} \nabla \right) p + \frac{\kappa^2}{\rho} p = 0 \tag{2}$$

where p is acoustic pressure and $\kappa = \omega/c + i\beta$ (complex) is a wave number.

Problem set: We have the partial differential equation(s) with boundary conditions that we want to solve.
Solution: The numerical modeling process is shown in Figure 1.
The numerical method that we are using is called the ultra weak variational formulation.

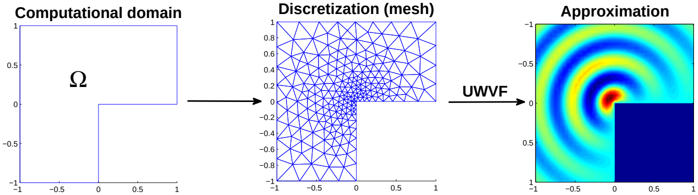

Figure: Solving process. First we have a computational domain. Second we discretize the computational domain (e.g. triangles). Third we solve problem using the UWVF.

Equations behind the solutions

Let us consider again the Helmholtz equation (2). Let Ω be a bounded domain in $\mathbb{R}^2$ with the boundary Γ and $\boldsymbol{n}$ the outward normal unit vector. The homogeneous time-harmonic Helmholtz problem is

$$\nabla \cdot \left(\frac{1}{\rho} \nabla \right) p + \frac{\kappa^2}{\rho} p = 0 \text{ in } \Omega \tag{3}$$

$$\left(\frac{1}{\rho} \frac{\partial p}{\partial \boldsymbol{n}} - i\sigma p \right) = Q \left(-\frac{1}{\rho} \frac{\partial p}{\partial \boldsymbol{n}} - i\sigma p \right) + g \text{ on } \Gamma \tag{4}$$

where p is a pressure, $\kappa = \frac{\omega}{c} \neq 0$ is a wave number, $Q \in \mathbb{C}$ with $|Q| \leq 1$ gives boundary conditions, $\sigma \in \mathbb{R}$ is a coupling parameter ($\sigma = \Re\{\kappa\}/\rho$) and g is the source term.
Boundary conditions:
$Q = 1$: Neumann b.c.
$Q = -1$: Dirichlet b.c.
$Q \neq 1, -1$: mixed, Robin b.c.

Finnish Centre of Excellence in Inverse Problems Research
UNIVERSITY OF EASTERN FINLAND

Sound-hard, rigid, scatterer

Let us assume that the computational domain Ω consists of two domains s.t. $\Omega = \Omega_1 \cup \Omega_2$, the interface between Ω_1 and Ω_2 is $\partial\Omega_1$ and $\rho_1 c_1 >> \rho_2 c_2$ (characteristic impedance). The total fiel is $p = p_i + p_s$ where p_i is incident field and p_s is scattered field. In addition, $\nabla^2 p_i + \kappa_2^2 p_i = 0$ in Ω_2.

Sound-hard, rigid, scatterer

Let us assume that the computational domain Ω consists of two domains s.t. $\Omega = \Omega_1 \cup \Omega_2$, the interface between Ω_1 and Ω_2 is $\partial\Omega_1$ and $\rho_1 c_1 >> \rho_2 c_2$ (characteristic impedance). The total fiel is $p = p_i + p_s$ where p_i is incident field and p_s is scattered field. In addition, $\nabla^2 p_i + \kappa_2^2 p_i = 0$ in Ω_2. We need to find p_s s.t.

$$\nabla^2 p_s + \kappa_2^2 p_s = 0 \quad \text{in } \Omega_2 \tag{5}$$

$$\frac{1}{\rho_2}\frac{\partial p_s}{\partial \boldsymbol{n}} = -\frac{1}{\rho_2}\frac{\partial p_i}{\partial \boldsymbol{n}} \quad \text{on } \partial\Omega_1 \tag{6}$$

$$\lim_{R\to\infty} R^{(d-1)/2}\left(\frac{\partial p_s}{\partial R} - i\kappa_2 p_s\right) = 0 \tag{7}$$

where d is the dimension of the problem and R is the distance.

Sound-hard, rigid, scatterer

Let us assume that the computational domain Ω consists of two domains s.t. $\Omega = \Omega_1 \cup \Omega_2$, the interface between Ω_1 and Ω_2 is $\partial\Omega_1$ and $\rho_1 c_1 >> \rho_2 c_2$ (characteristic impedance). The total fiel is $p = p_i + p_s$ where p_i is incident field and p_s is scattered field. In addition, $\nabla^2 p_i + \kappa_2^2 p_i = 0$ in Ω_2. We need to find p_s s.t.

$$\nabla^2 p_s + \kappa_2^2 p_s = 0 \quad \text{in } \Omega_2 \tag{5}$$

$$\frac{1}{\rho_2}\frac{\partial p_s}{\partial \boldsymbol{n}} = -\frac{1}{\rho_2}\frac{\partial p_i}{\partial \boldsymbol{n}} \quad \text{on } \partial\Omega_1 \tag{6}$$

$$\lim_{R\to\infty} R^{(d-1)/2}\left(\frac{\partial p_s}{\partial R} - i\kappa_2 p_s\right) = 0 \tag{7}$$

where d is the dimension of the problem and R is the distance. Equation (7) is Sommerfeld radiation condition i.e. scattered field propagates away from the volume V_1 and vanishes when $R \to \infty$.

Sound-soft, pressure release, scatterer

Let us assume that the computational domain Ω consists of two domains s.t. $\Omega = \Omega_1 \cup \Omega_2$, the interface between Ω_1 and Ω_2 is $\partial\Omega_1$ and $\rho_1 c_1 << \rho_2 c_2$ (characteristic impedance). The total fiel is $p = p_i + p_s$ where p_i is incident field and p_s is scattered field. In addition, $\nabla^2 p_i + \kappa_2^2 p_i = 0$ in Ω_2.

Sound-soft, pressure release, scatterer

Let us assume that the computational domain Ω consists of two domains s.t. $\Omega = \Omega_1 \cup \Omega_2$, the interface between Ω_1 and Ω_2 is $\partial\Omega_1$ and $\rho_1 c_1 << \rho_2 c_2$ (characteristic impedance). The total fiel is $p = p_i + p_s$ where p_i is incident field and p_s is scattered field. In addition, $\nabla^2 p_i + \kappa_2^2 p_i = 0$ in Ω_2. We need to find p_s s.t.

$$\nabla^2 p_s + \kappa_2^2 p_s = 0 \quad \text{in } \Omega_2 \tag{8}$$

$$p_s = -p_i \quad \text{on } \partial\Omega_1 \tag{9}$$

$$\lim_{R\to\infty} R^{(d-1)/2} \left(\frac{\partial p_s}{\partial R} - i\kappa_2 p_s \right) = 0 \tag{10}$$

where d is the dimension of the problem and R is the distance. Equation (10) is Sommerfeld radiation condition.

Local acoustic absorbing boundary condition

Local acoustic absorbing boundary condition (ABC), zeroth order absorbing boundary condition, is of the form

$$\frac{\partial p}{\partial \boldsymbol{n}} - i\kappa p = 0 \quad \text{on exterior boundary } \Gamma \tag{11}$$

that is obtained from Sommerfeld radiation condition.
Zeroth order ABC may suffer from poor accuracy in some problems.

Perfectly mathced layer

Perfectly matched layer (PML) was introduced by Bérenger for electromagnetic problems and it has been applied also in acoustics. The PML for inhomogeneous Helmholtz equation can be derived using complex streching variables, i.e.

$$x' = \begin{cases} x + \frac{i}{\kappa} \int_x^{x_0} \sigma_{0,x}(|x| - x_0)^n dx & |x| \geq x_0 \\ x & |x| < x_0 \end{cases}$$

$$y' = \begin{cases} y + \frac{i}{\kappa} \int_y^{y_0} \sigma_{0,y}(|y| - y_0)^n dy & |y| \geq y_0 \\ y & |y| < y_0 \end{cases}$$

$$z' = \begin{cases} z + \frac{i}{\kappa} \int_z^{z_0} \sigma_{0,z}(|z| - z_0)^n dz & |z| \geq z_0 \\ z & |z| < z_0 \end{cases}$$

where $\sigma_{0,x}, \sigma_{0,y}, \sigma_{0,z}$ are constants and n is the integer.

In addition, we can write

$$d_x(x) := \frac{\partial x'}{\partial x} = \begin{cases} 1 + \frac{i}{\kappa}\sigma_{0,x}(|x| - x_0)^n & |x| \geq x_0 \\ 1 & |x| < x_0 \end{cases}$$

$$d_y(y) := \frac{\partial y'}{\partial y} = \begin{cases} 1 + \frac{i}{\kappa}\sigma_{0,y}(|y| - y_0)^n & |y| \geq y_0 \\ 1 & |y| < y_0 \end{cases}$$

$$d_z(z) := \frac{\partial z'}{\partial z} = \begin{cases} 1 + \frac{i}{\kappa}\sigma_{0,z}(|z| - z_0)^n & |z| \geq z_0 \\ 1 & |z| < z_0 \end{cases}$$

Straightforward derivation leads

$$\nabla \cdot \left(\frac{1}{\rho} A \nabla \right) p + \frac{\kappa^2 \eta^2}{\rho} p = f_s \eta^2 \qquad (12)$$

where $\eta^2 = d_x d_y d_z$ and $A = \mathrm{diag}(\frac{d_y d_z}{d_x}, \frac{d_x d_z}{d_y}, \frac{d_x d_y}{d_z})$

Performance of the UWVF in acoustics

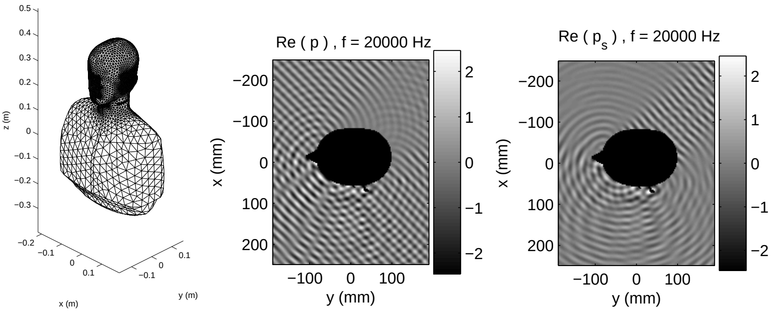

Figure: Modeling of head-related transfer function (HRTF). Left: Total pressure at 20 kHz. Right: Scattered pressure at 20 kHz. Reference: Huttunen, Seppälä, Kärkkäinen, Kärkkäinen: Simulation of the transfer function for a head-and-torso model over the entire audible frequency range, Journal of Computational Acoustics, Volume: 15, Issue: 4(2007) pp. 429-448.

Anisotropic Helmholtz problem using PML

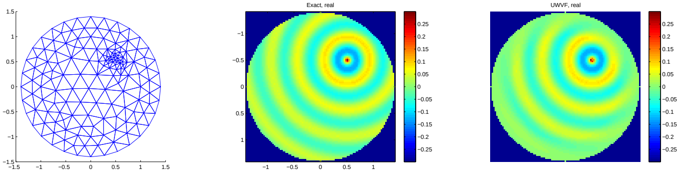

Figure: Anisotropic Helmholtz problem with UWVF using PML (error = 2.2318%).

Anisotropic Helmholtz problem using ABC

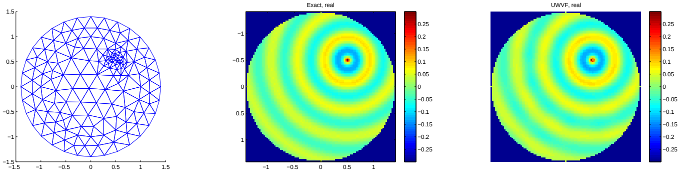

Figure: Anisotropic Helmholtz problem with UWVF using zeroth order ABC (error = 7.9381%).

Scattering from a circle

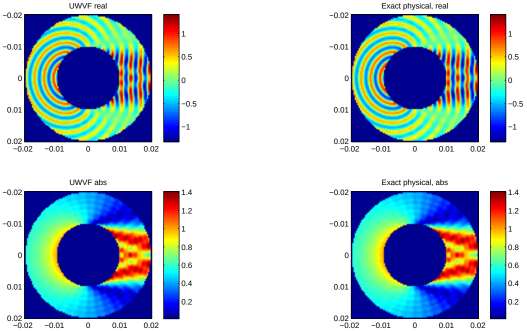

Figure: Scattering from a circle (sound-hard scatterer).

- Results shown earlier were computed using the ultra weak variational formulation (UWVF). However, at first we shall look at the finite element method that is widely used in modeling problems. Properties of FEM will be discussed shortly.
- Note: The UWVF and FEM are different methods even though they both use finite elements (e.g. triangles, tetrahedra)
- Next we shall show the weak formulation of Helmholtz problem

Weak form in FEM

Weak formulation: We multiply Helmholtz equation (3) by a test function $v \in H^1(\Omega)$ (Sobolev space) and integrate over the computational domain Ω. Hence

$$\int_\Omega \left[\nabla \cdot \left(\frac{1}{\rho} \nabla \right) p + \frac{\kappa^2}{\rho} p \right] v = 0 \tag{13}$$

Weak form in FEM

Weak formulation: We multiply Helmholtz equation (3) by a test function $v \in H^1(\Omega)$ (Sobolev space) and integrate over the computational domain Ω. Hence

$$\int_\Omega \left[\nabla \cdot \left(\frac{1}{\rho} \nabla \right) p + \frac{\kappa^2}{\rho} p \right] v = 0 \tag{13}$$

Integration by parts gives

$$-\int_\Omega \frac{1}{\rho} \nabla p \cdot \nabla v + \int_\Gamma \frac{1}{\rho} \frac{\partial p}{\partial \boldsymbol{n}} v + \int_\Omega \frac{\kappa^2}{\rho} p v = 0 \tag{14}$$

The boundary condition (4) can be written as

$$\frac{1}{\rho}\frac{\partial p}{\partial \boldsymbol{n}} = \frac{1-Q}{1+Q} i\sigma p + \frac{1}{1+Q} g. \tag{15}$$

The boundary condition (4) can be written as

$$\frac{1}{\rho}\frac{\partial p}{\partial \boldsymbol{n}} = \frac{1-Q}{1+Q} i\sigma p + \frac{1}{1+Q} g. \tag{15}$$

Plugging equation (15) into the equation (14) and rearranging terms we obtain

$$-\int_\Omega \frac{1}{\rho}\nabla p \cdot \nabla v + \int_\Omega \frac{\kappa^2}{\rho} pv + \int_\Gamma \frac{1-Q}{1+Q} i\sigma pv = -\int_\Gamma \frac{1}{1+Q} gv \tag{16}$$

The bilinear form is

$$a(p,v) = -\int_\Omega \frac{1}{\rho}\nabla p \cdot \nabla v + \int_\Omega \frac{\kappa^2}{\rho} pv + \int_\Gamma \frac{1-Q}{1+Q} i\sigma pv \tag{17}$$

and the RHS is

$$F(v) = -\int_\Gamma \frac{1}{1+Q} gv. \tag{18}$$

Variational problem

We want to find $p \in H^1(\Omega)$ s.t.

$$a(p, v) = F(v) \tag{19}$$

for all $v \in H^1(\Omega)$.

About the FEM

- Widely used for solving physical problems (which include partial differential equations)
- Handles complex geometries and inhomogeneous media
- Discretization using piecewise polynomial basis functions
- Accuracy obtained by increasing the polynomial order and/or number of elements
- Low-order FEM needs 10 grid points per wavelength and at higher wave numbers even more discretization points are needed due to the "numerical pollution" error
  $\Rightarrow$ Computational burden increases more and more when wave number grows

About the FEM continues

- Low-order FEM needs 10 grid points per wavelength and at higher wave numbers even more discretization points are needed due to the "numerical pollution" error
$\Rightarrow$ Computational burden increases more and more when wave number grows
- For low-order FEM the error estimate is of the form

$$\text{error} = C_1 \kappa h + C_2 \kappa^3 h^2 \tag{20}$$

where κ is the wave number, h is the element size and C_1, C_2 are constants.
- Non-polynomial methods have been found to be competitive to standard FEMs

Non-polynomial basis methods

- The partition of unity finite element method (PUFEM) by Babuška and Melenk (1997).
- Least squares method (LSM) by Monk and Wang (1999).
- Discontinuous enrichment method (DEM) by Farhat et al. (2001).
- Discontinuous Galerkin method (DGM) by Farhat et al. (2003), Gittelson, Hiptmair and Perugia (2007).
- Discontinuous Petrov-Galerkin method (DPGM) by Demkowicz et al. (2009)
- Non-polynomial FEM by Barnett and Betcke (2009)
- The ultra-weak variational formulation (UWVF) by Després (1994), Cessenat and Després (1998).

The UWVF

- Special form of the DGM, Huttunen, Malinen and Monk (2006), Gabard (2007)
- Competitive method to FEM
- Volume based method and uses FE meshes
- Basis discontinuous over elements, physical basis functions e.g. plane waves
  - plane wave basis $\Rightarrow$ integrals can be computed efficiently in closed form
  - allows to define different number of basis functions for different wave components
  - number of basis functions can vary from element to element
- Matrices resulting in the UWVF are sparse

What affects accuracy in the UWVF?

- The number of basis functions per element (too many basis functions per element may produce an ill-conditioned system)
- The ratio between basis function components in elasticity (P-,SH- and SV-waves)
- Mesh size
- The choice of numerical flux between elements (next two slides)

Uniform mesh

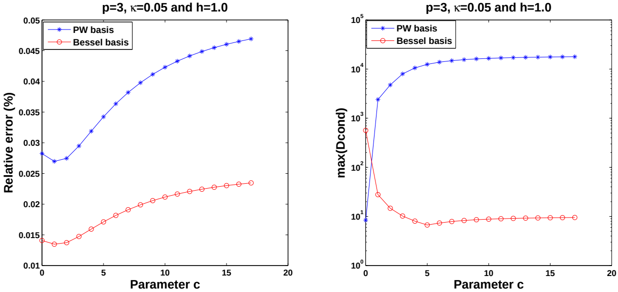

Figure: Results for $\kappa = 0.05$ when $p = 3$, $h = 1.0$ and a coupling parameter is $\sigma = (\kappa + c/h)$. Parameter c varies.

Uniform mesh

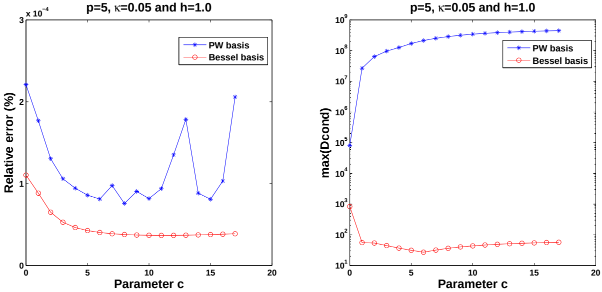

Figure: Results for $\kappa = 0.05$ when $p = 5$, $h = 1.0$ and a coupling parameter is $\sigma = (\kappa + c/h)$. Parameter c varies.

Notations

The ultra weak variational formulation for the Helmholtz problem (3)-(4) is derived next.

Part of the mesh. Exterior boundary of an element Ω_k is denoted by Γ_k and outward unit normal by $\boldsymbol{n}_k$. The interface between elements Ω_k and Ω_j is denoted as $\sum_{k,j}$.

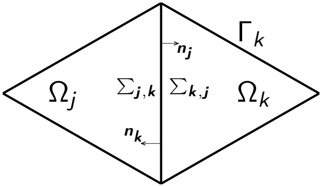

Let p_k satisfy the Helmholtz equation

$$\Delta p_k + \kappa_k^2 p_k = 0 \quad \text{in } \Omega_k. \tag{21}$$

We assume that smooth test function v_k satisfy the adjoint Helmholtz equation, i.e.

$$\Delta \overline{v}_k + \kappa_k^2 \overline{v}_k = 0 \quad \text{in } \Omega_k. \tag{22}$$

We can write the following equation

$$\sum_{k=1}^{N}\int_{\partial\Omega_k}\frac{1}{\sigma}\left(-\frac{1}{\rho_k}\frac{\partial p_k}{\boldsymbol{n}_k}-i\sigma p_k\right)\overline{\left(-\frac{1}{\rho_k}\frac{\partial v_k}{\boldsymbol{n}_k}-i\sigma v_k\right)}$$
$$=\sum_{k=1}^{N}\int_{\partial\Omega_k}\frac{1}{\sigma}\left(\frac{1}{\rho_k}\frac{\partial p_k}{\boldsymbol{n}_k}-i\sigma p_k\right)\overline{\left(\frac{1}{\rho_k}\frac{\partial v_k}{\boldsymbol{n}_k}-i\sigma v_k\right)}$$
$$-\sum_{k=1}^{N}2\frac{i}{\rho_k}\int_{\partial\Omega_k}\left(\frac{\partial p_k}{\partial\boldsymbol{n}_k}\overline{v}_k-p_k\frac{\partial\overline{v}_k}{\partial\boldsymbol{n}_k}\right) \qquad (23)$$

for all smooth test functions v_k.

Using Green's identity we can write

$$\int_{\partial\Omega_k} \left(\frac{\partial p_k}{\partial \boldsymbol{n}_k} \overline{v}_k - p_k \frac{\partial \overline{v}_k}{\partial \boldsymbol{n}_k} \right) = \int_{\Omega_k} \left(\Delta p_k \overline{v}_k - p_k \Delta \overline{v}_k \right) \tag{24}$$

On the other hand, from equations (21) and (22) we know that

$$\Delta p_k = -\kappa_k^2 p_k \quad \text{and} \quad \Delta \overline{v}_k = -\kappa_k^2 \overline{v}_k.$$

Therefore

$$\int_{\Omega_k} \left(\Delta p_k \overline{v}_k - p_k \Delta \overline{v}_k \right) = \int_{\Omega_k} \left(-\kappa_k^2 p_k \overline{v}_k + p_k \kappa_k^2 \overline{v}_k \right) = 0 \tag{25}$$

Hence, we obtain

$$\begin{aligned}\sum_{k=1}^{N}\int_{\partial\Omega_k}\frac{1}{\sigma}\left(-\frac{1}{\rho_k}\frac{\partial p_k}{\boldsymbol{n}_k}-i\sigma p_k\right)\overline{\left(-\frac{1}{\rho_k}\frac{\partial v_k}{\boldsymbol{n}_k}-i\sigma v_k\right)}\\ =\sum_{k=1}^{N}\int_{\partial\Omega_k}\frac{1}{\sigma}\left(\frac{1}{\rho_k}\frac{\partial p_k}{\boldsymbol{n}_k}-i\sigma p_k\right)\overline{\left(\frac{1}{\rho_k}\frac{\partial v_k}{\boldsymbol{n}_k}-i\sigma v_k\right)}\end{aligned} \tag{26}$$

Notice that on the interior interfaces the following conditions must hold, also coupling forms (transmission conditions),

$$p_k = p_j \quad \text{on} \sum_{k,j} \tag{27}$$

$$\frac{\partial p_k}{\partial \boldsymbol{n}_k} = -\frac{\partial p_j}{\partial \boldsymbol{n}_j} \quad \text{on} \sum_{k,j}. \tag{28}$$

Defining a new function

$$\mathcal{X}_k = \left(-\frac{1}{\rho_k} \frac{\partial p_k}{\partial \boldsymbol{n}_k} - i\sigma p_k \right) \Bigg|_{\partial \Omega_{\boldsymbol{k}}}, \quad k = 1, \dots, N. \tag{29}$$

Substituting the boundary condition (4) and sufficient coupling forms (transmission conditions) of (27)-(28) to the (26) and using new function (29) we obtain

$$\sum_{k=1}^{N} \int_{\partial\Omega_{\boldsymbol{k}}} \frac{1}{\sigma} \mathcal{X}_k \overline{\left(-\frac{1}{\rho_k} \frac{\partial v_k}{\partial \boldsymbol{n}_k} - i\sigma v_k \right)} \mathrm{d}A - \sum_{k=1}^{N} \sum_{j=1}^{N} \int_{\Sigma_{\boldsymbol{k},\boldsymbol{j}}} \frac{1}{\sigma} \mathcal{X}_j \overline{\left(\frac{1}{\rho_k} \frac{\partial v_k}{\partial \boldsymbol{n}_k} - i\sigma v_k \right)} \mathrm{d}A$$
$$- \sum_{k=1}^{N} \int_{\Gamma_{\boldsymbol{k}}} \frac{Q}{\sigma} \mathcal{X}_k \overline{\left(\frac{1}{\rho_k} \frac{\partial v_k}{\partial \boldsymbol{n}_k} - i\sigma v_k \right)} \mathrm{d}A = \sum_{k=1}^{N} \int_{\Gamma_{\boldsymbol{k}}} \frac{1}{\sigma} g \overline{\left(\frac{1}{\rho_k} \frac{\partial v_k}{\partial \boldsymbol{n}_k} - i\sigma v_k \right)} \mathrm{d}A,$$

for all v_k satisfying the adjoint Helmholtz equation (22).

To simplify notations we denote

$$F_k(\mathcal{Y}_k) = \left(\frac{1}{\rho_k}\frac{\partial v_k}{\partial \boldsymbol{n}_k} - i\sigma v_k\right) \quad \text{on } \partial\Omega_k \tag{30}$$

and

$$\mathcal{Y}_k = \left(-\frac{1}{\rho_k}\frac{\partial v_k}{\partial \boldsymbol{n}_k} - i\sigma v_k\right) \quad \text{on } \partial\Omega_k \tag{31}$$

Then the UWVF can be written as

$$\sum_{k=1}^{N}\int_{\partial\Omega_k}\frac{1}{\sigma}\mathcal{X}_k\overline{\mathcal{Y}_k}\mathrm{d}A - \sum_{k=1}^{N}\sum_{j=1}^{N}\int_{\Sigma_{k,j}}\frac{1}{\sigma}\mathcal{X}_j\overline{F_k(\mathcal{Y}_k)}\mathrm{d}A \tag{32}$$

$$-\sum_{k=1}^{N}\int_{\Gamma_k}\frac{Q}{\sigma}\mathcal{X}_k\overline{F_k(\mathcal{Y}_k)}\mathrm{d}A = \sum_{k=1}^{N}\int_{\Gamma_k}\frac{1}{\sigma}g\overline{F_k(\mathcal{Y}_k)}\mathrm{d}A, \tag{33}$$

Discretization

We choose finite family of functions $\varphi_{k,\ell}$, $\ell = 1, \ldots, N_k$ for each Ω_k that satisfy the adjoint Helmholtz equation (22). Hence

$$\mathcal{Y}_k^a = \sum_{k=1}^{N_k} \mathcal{Y}_{k,\ell} \left(-\frac{1}{\rho_k} \frac{\partial \varphi_{k,\ell}}{\partial \boldsymbol{n}_k} - i\sigma\varphi_{k,\ell} \right) \quad k = 1, \ldots, N \tag{34}$$

Similarly

$$\mathcal{X}_k^a = \sum_{k=1}^{N_k} \mathcal{X}_{k,\ell} \left(-\frac{1}{\rho_k} \frac{\partial \varphi_{k,\ell}}{\partial \boldsymbol{n}_k} - i\sigma\varphi_{k,\ell} \right) \quad k = 1, \ldots, N \tag{35}$$

and

$$F_k(\mathcal{Y}_k^a) = \sum_{k=1}^{N_k} \mathcal{Y}_{k,\ell} \left(\frac{1}{\rho_k} \frac{\partial \varphi_{k,\ell}}{\partial \boldsymbol{n}_k} - i\sigma\varphi_{k,\ell} \right) \quad k = 1, \ldots, N \tag{36}$$

Using now (34)-(36) in equation (33) we obtain the discrete UWVF.

In matrix form

$$\left(\mathbf{D}-\mathbf{C}\right)\mathbf{X}=\mathbf{b}\Rightarrow\left(\mathbf{I}-\mathbf{D}^{-1}\mathbf{C}\right)\mathbf{X}=\mathbf{D}^{-1}\mathbf{b}. \tag{37}$$

Matrix D is a Hermitian block diagonal i.e. $D=\mathrm{diag}(D_1,\dots,D_N)$. Let us write the form of the entries

$$D_k^{\ell,m}=\int_{\partial\Omega_k}\frac{1}{\sigma}\left(-\frac{1}{\rho_k}\frac{\partial\varphi_{k,m}}{\partial\boldsymbol{n}_k}-i\sigma\varphi_{k,m}\right)\overline{\left(-\frac{1}{\rho_k}\frac{\partial\varphi_{k,m}}{\partial\boldsymbol{n}_k}-i\sigma\varphi_{k,m}\right)} \tag{38}$$

The matrix C entries are

$$C_{k,j}^{\ell,m}=\int_{\sum_{k,j}}\frac{1}{\sigma}\left(\frac{1}{\rho_j}\frac{\partial\varphi_{j,m}}{\partial\boldsymbol{n}_k}-i\sigma\varphi_{j,m}\right)\overline{\left(\frac{1}{\rho_k}\frac{\partial\varphi_{k,\ell}}{\partial\boldsymbol{n}_k}-i\sigma\varphi_{k,\ell}\right)} \tag{39}$$

$$+\int_{\sum_{k,j}}\frac{Q}{\sigma}\left(-\frac{1}{\rho_k}\frac{\partial\varphi_{k,m}}{\partial\boldsymbol{n}_k}-i\sigma\varphi_{k,m}\right)\overline{\left(\frac{1}{\rho_k}\frac{\partial\varphi_{k,\ell}}{\partial\boldsymbol{n}_k}-i\sigma\varphi_{k,\ell}\right)} \tag{40}$$

The RHS vector b can be constructed from

$$b_k^\ell = \int_{\Gamma_k} \frac{1}{\rho} g \overline{\left(\frac{1}{\rho_k} \frac{\partial \varphi_{k,\ell}}{\partial \boldsymbol{n}_k} - i\sigma \varphi_{k,\ell} \right)} \qquad (41)$$

Plane wave (PW) basis

$$\varphi_{k,\ell} = \begin{cases} \exp\left(i\overline{\kappa}_k d_{k,\ell} \cdot \underline{x}_k\right) \text{ in } \Omega_k \\ 0, \text{ elsewhere} \end{cases}$$

in which the direction $d_{k,\ell} = \left(\cos\left(2\pi \frac{\ell-1}{N_k}\right), \sin\left(2\pi \frac{\ell-1}{N_k}\right)\right)$.

Pros and cons of PW basis

- The UWVF integrals can be computed in a closed form
- $\Rightarrow$ Efficient to compute.
- Ill-conditioning may occur when elements are small or at low frequencies.
- May have challenges with sharp corners

Bessel basis with scaling is of the form

$$\varphi_{k,\ell} = \begin{cases} \frac{J_\ell(\overline{\kappa}_k|\underline{x}_k - \underline{x}_{0,k}|)}{J_\ell(\overline{\kappa}_k h_k)} e^{i\ell\theta} & \text{in } \Omega_k \\ 0, & \text{elsewhere} \end{cases}$$

where h_k is the edge of an element, $\underline{x}_{0,k}$ is the "basis origin" and θ is an angle. Bessel basis without scaling is

$$\varphi_{k,\ell} = \begin{cases} J_\ell(\overline{\kappa}_k|\underline{x}_k - \underline{x}_{0,k}|) e^{i\ell\theta} & \text{in } \Omega_k \\ 0, & \text{elsewhere} \end{cases}$$

the order of Bessel function ℓ in an element Ω_k is

$$\ell = s - \frac{p_k - 1}{2} - 1$$

where $s = 1, \ldots, p_k$.

Pros and cons of Bessel basis

- The UWVF integrals must be computed using quadratures
- Slower to compute than PW basis
- Condition number is smaller for the scaled Bessel basis than it is using PW basis at low frequencies or when element sizes are small
- Help singularities

We seek the solution to the problem

$$\Delta u + \kappa^2 u = 0 \text{ in } \Omega$$
$$\frac{\partial u}{\partial \boldsymbol{n}} + i\sigma u = \frac{\partial g}{\partial \boldsymbol{n}} + i\sigma g \text{ on } \Gamma$$

where $g = \exp(i\kappa d \cdot x)$
and $d = (\cos(\pi/p), \sin(\pi/p))$
for plane wave propagation
and $g = \exp(i(\alpha_1(x+1) + \alpha_2 y))$
where $\alpha_1^2 + \alpha_2^2 = \kappa^2$,
$\alpha_1 = i\kappa\sqrt{\beta^2 - 1}$ and $\alpha_2 = \beta\kappa$
with $\beta > 1$ for evanescent wave.

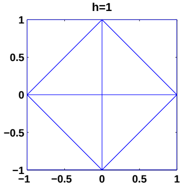

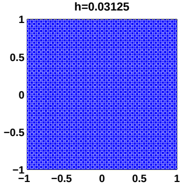

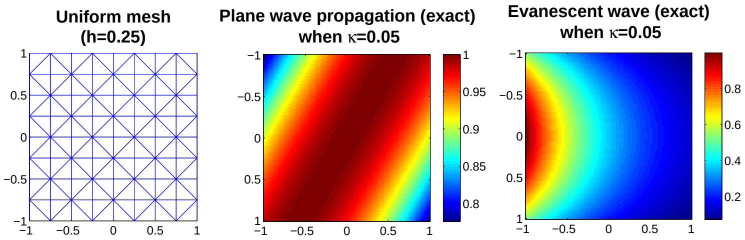

Figure: One of the meshes on the LHS. The exact solution for the plane wave propagation problem (center) is $u_{ex} = \exp(i\kappa \underline{d} \cdot \underline{x})$ and for the evanescent wave problem (RHS) $u_{ex} = \exp(i(\alpha_1(x+1) + \alpha_2 y))$ where $\alpha_1^2 + \alpha_2^2 = \kappa^2$, $\alpha_1 = i\kappa\sqrt{\beta^2 - 1}$ and $\alpha_2 = \beta\kappa$ with $\beta > 1$.

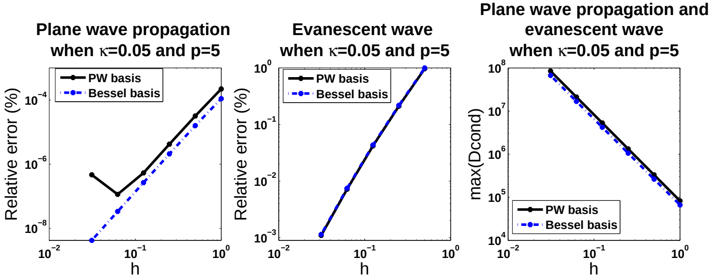

Figure: Relative error (%) vs. the mesh size h for plane wave propagation (LHS) and evanescent wave (center) and the condition number of matrix $\mathbf{D}$ vs. mesh size (RHS).

Approximate u that satisfies

$$\Delta u + \kappa^2 u = 0 \text{ in } \Omega$$
$$u = 0 \text{ on } \Gamma_1$$
$$\frac{\partial u}{\partial \boldsymbol{n}} + i\sigma u = \frac{\partial g}{\partial \boldsymbol{n}} + i\sigma g \text{ on } \Gamma_2$$

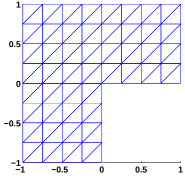

where

$$g(r,\theta) = J_{\frac{2}{3}}(\kappa r)\sin(\frac{2}{3}\theta).$$

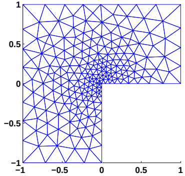

The exact solution
to the L-shaped domain problem
is $u_{ex} = g$. This solution has
a singular derivative at the origin.

In simulations we use regular plane wave basis and Bessel basis. We can use modified Bessel basis in which we take into account the exact solution. The modified Bessel basis is of the form

$$\varphi_{k,\ell} = \begin{cases} J_{|\ell|}(\overline{\kappa}_k|\underline{x}_k - \underline{x}_{0,k}|)e^{i\ell\theta} \text{ in } \Omega_k \text{ and if } \ell = -2/3 \\ J_{\ell}(\overline{\kappa}_k|\underline{x}_k - \underline{x}_{0,k}|)e^{i\ell\theta} \text{ in } \Omega_k \text{ and if } \ell \neq -2/3 \\ 0, \text{ elsewhere} \end{cases}$$

the order of Bessel function ℓ in an element Ω_k is

$$\ell = \begin{cases} s - \frac{p_k-3}{2} - 1, \text{ when } s = 1, \dots, p_k - 2 \\ \frac{2}{3}, \text{ when } s = p_k - 1 \\ -\frac{2}{3}, \text{ when } s = p_k \end{cases}$$

PW-Bessel-UWVF in an L-shaped domain (uniform).

We use modified Bessel basis in elements which lie near the singular point (in 5 elements) and elsewhere we use regular plane wave basis.

Table: Results using PW+Bessel basis functions in an uniform mesh.

Basis	κ	p	error(%)	max(Dcond)	CPU Time [s]
PW+Bessel	0.05	5	1.0827	1.3196e6	20.7810
	0.5	5	0.2498	1.3132e4	20.7004
	5	7	0.1194	4.7782e3	35.4461
	50	25	0.0246	2.6588e7	747.6763

Basis	κ	p	error(%)	max(Dcond)	CPU Time [s]
PW	0.05	5	1.5173	1.3196e6	7.7368
	0.5	5	1.0571	1.3132e4	7.6037
	5	7	1.8760	4.7782e3	10.6958
	50	25	2.8962	3.3511e5	73.4306

PW-Bessel-UWVF in an L-shaped domain (non-uniform).

Choosing the number of basis functions in a non-uniform mesh can be obtained from

$$p_k = \mathtt{round}(\kappa_k h_k + C(\kappa_k h_k)^{1/3})$$

where h is the edge of the element, C is a constant ($C = 5$ in our simulations below) and if p_k is even we set $p_k = p_k - 1$.

PW-Bessel-UWVF in an L-shaped domain (non-uniform).

Table: Results using PW+Bessel basis functions for the non-uniform mesh.

Basis	κ	p	error(%)	max(Dcond)	CPU Time [s]
PW+Bessel	0.05	3	2.3529	65.0767	25.3846
	0.5	3	0.4960	14.3588	25.4662
	5	3...7	1.8532	2.3514e4	33.2713
	50	7..27	0.0454	1.2786e8	210.9513
Basis	κ	p	error(%)	max(Dcond)	CPU Time [s]
PW	0.05	3	0.4999	11.2229	14.9222
	0.5	3	0.4791	11.1942	17.3626
	5	3...7	2.6257	2.3514e4	21.7997
	50	7..27	2.1779	1.2786e8	161.4971

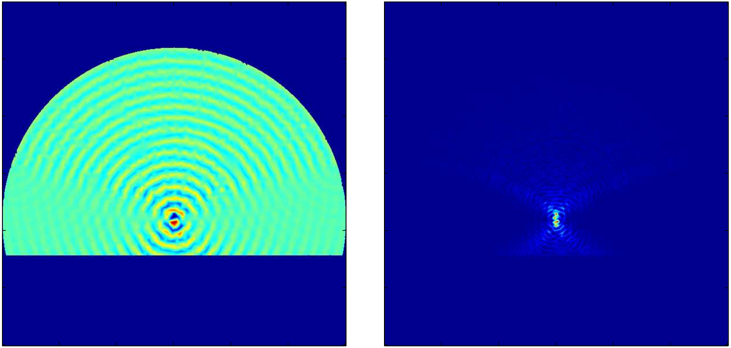

Figure: Fluid medium.

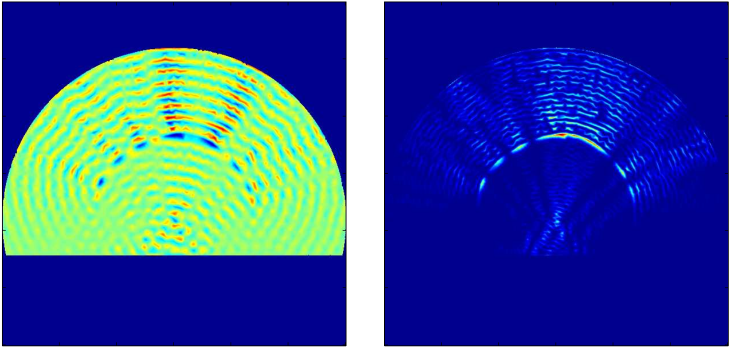

Figure: Fluid brain.

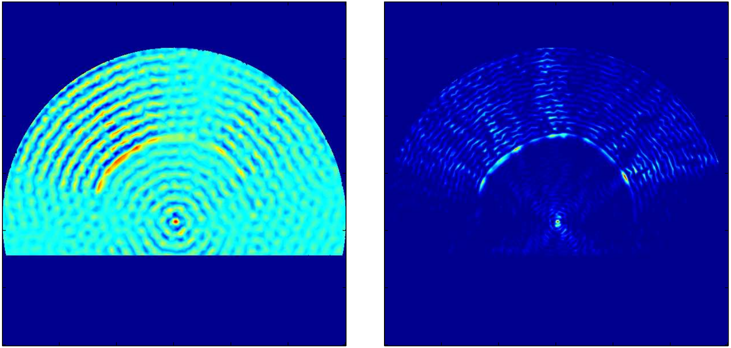

Figure: Example of modeling focused ultrasound of brain.

Navier equation

Let Ω be a computational domain with the boundary $\Gamma = \partial\Omega$ and let Ω consists of non-overlapping elements, i.e. $\Omega = \cup_{k=1}^{N}\Omega_k$ where N is the number of elements. For each Ω_k the Navier equation is

$$\mu\Delta\mathbf{u} + (\lambda+\mu)\nabla(\nabla\cdot\mathbf{u}) + \omega^2\rho\mathbf{u} = 0 \quad \text{in } \Omega_k \tag{42}$$

where ω is the angular frequency of the field, $\mathbf{u}$ is the time-harmonic displacement vector, λ and μ are the Lamé constants and ρ is the density of the medium.

Lamé constants and wave speeds

The Lamé constants can be expressed as

$$\mu = \frac{E}{2(1-\nu)}, \quad \lambda = \frac{E\nu}{(1+\nu)(1-2\nu)}, \tag{43}$$

where E is the Young's modulus and ν is the Poisson ratio. The wave speeds for the P-wave and S-wave are,

$$c_P = \sqrt{\frac{\lambda+2\mu}{\rho}}, \qquad c_S = \sqrt{\frac{\mu}{\rho}}. \tag{44}$$

Traction operator

Traction operator $\mathbf{T}^{(\mathbf{n})}(\mathbf{u})$ maps local displacements to local tractions on any closed surface S and it is defined as

$$\mathbf{T}^{(\mathbf{n})}(\mathbf{u}) = 2\mu \frac{\partial \mathbf{u}}{\partial \mathbf{n}} + \lambda \mathbf{n} \nabla \cdot \mathbf{u} + \mu \mathbf{n} \times \nabla \times \mathbf{u}. \tag{45}$$

where $\mathbf{n}$ is an outward unit normal to the surface S.

Traction operator

Traction operator $\mathbf{T}^{(\mathbf{n})}(\mathbf{u})$ maps local displacements to local tractions on any closed surface S and it is defined as

$$\mathbf{T}^{(\mathbf{n})}(\mathbf{u}) = 2\mu\frac{\partial \mathbf{u}}{\partial \mathbf{n}} + \lambda \mathbf{n}\nabla \cdot \mathbf{u} + \mu \mathbf{n} \times \nabla \times \mathbf{u}. \qquad (45)$$

where $\mathbf{n}$ is an outward unit normal to the surface S. In addition, the complex conjugate of the traction operator $\mathbf{T}$ is

$$\overline{\mathbf{T}^{(\mathbf{n})}}(\mathbf{u}) = 2\overline{\mu}\frac{\partial \mathbf{u}}{\partial \mathbf{n}} + \overline{\lambda} \mathbf{n}\nabla \cdot \mathbf{u} + \overline{\mu} \mathbf{n} \times \nabla \times \mathbf{u} \qquad (46)$$

and $\overline{\overline{\mathbf{T}^{(\mathbf{n})}}(\mathbf{u})} = \mathbf{T}^{(\mathbf{n})}(\overline{\mathbf{u}})$.

Faces and exterior boundary

Let Ω_k and Ω_j be neighboring elements and share a common face. The interface between Ω_k and Ω_j is denoted by $\sum_{k,j}$. Therefore on $\sum_{k,j}$ the following conditions hold

$$\mathbf{u}|_{\Omega_k} = \mathbf{u}|_{\Omega_j} \tag{47}$$

$$\mathbf{T}^{(\mathbf{n}|_{\Omega_k})}(\mathbf{u}|_{\Omega_k}) = -\mathbf{T}^{(\mathbf{n}|_{\Omega_j})}(\mathbf{u}|_{\Omega_j}) \tag{48}$$

where $\mathbf{n}|_{\Omega_k}$ is an outward normal to Ω_k and similarly $\mathbf{n}|_{\Omega_j}$ to Ω_j (note that $\mathbf{n}|_{\Omega_k} = -\mathbf{n}|_{\Omega_j}$).

Faces and exterior boundary

Let Ω_k and Ω_j be neighboring elements and share a common face. The interface between Ω_k and Ω_j is denoted by $\sum_{k,j}$. Therefore on $\sum_{k,j}$ the following conditions hold

$$\mathbf{u}|_{\Omega_k} = \mathbf{u}|_{\Omega_j} \tag{47}$$

$$\mathbf{T}^{(\mathbf{n}|_{\Omega_k})}(\mathbf{u}|_{\Omega_k}) = -\mathbf{T}^{(\mathbf{n}|_{\Omega_j})}(\mathbf{u}|_{\Omega_j}) \tag{48}$$

where $\mathbf{n}|_{\Omega_k}$ is an outward normal to Ω_k and similarly $\mathbf{n}|_{\Omega_j}$ to Ω_j (note that $\mathbf{n}|_{\Omega_k} = -\mathbf{n}|_{\Omega_j}$). On the exterior boundary Γ we have

$$\mathbf{T}^{(\mathbf{n})}(\mathbf{u}) - i\sigma\mathbf{u} = Q(-\mathbf{T}^{(\mathbf{n})}(\mathbf{u}) - i\sigma\mathbf{u}) + g \quad \text{on } \Gamma \tag{49}$$

where g is the source term, Q specifies the boundary conditions and σ is a coupling parameter (flux parameter).

Isometry Lemma

It can be shown that

$$\sum_k \int_{\partial\Omega_k} \sigma^{-1} \left(-\mathbf{T}^{(\mathbf{n}_k)}(\mathbf{u}_k) - i\sigma\mathbf{u}_k\right) \cdot \overline{\left(-\overline{\mathbf{T}^{(\mathbf{n}_k)}}(\mathbf{e}_k) - i\sigma\mathbf{e}_k\right)}$$
$$= \sum_k \int_{\partial\Omega_k} \sigma^{-1} \left(\mathbf{T}^{(\mathbf{n}_k)}(\mathbf{u}_k) - i\sigma\mathbf{u}_k\right) \cdot \overline{\left(\overline{\mathbf{T}^{(\mathbf{n}_k)}}(\mathbf{e}_k) - i\sigma\mathbf{e}_k\right)} \quad (50)$$

where $\mathbf{u}_k$ is the solution of the Navier equation (42) and $\mathbf{e}_k$ is the test function that satisfies the adjoint Navier's equation.

The UWVF

Using the "Isometry Lemma" and boundary conditions we obtain the UWVF as

$$\sum_k \int_{\partial\Omega_{\boldsymbol{k}}} \sigma^{-1} \mathcal{X}_k \cdot \overline{(-\overline{\mathbf{T}^{(\mathbf{n}_k)}}(\mathbf{e}_k) - i\sigma \mathbf{e}_k)} - \sum_k \sum_j \int_{\Sigma_{\boldsymbol{k},\boldsymbol{j}}} \sigma^{-1} \mathcal{X}_j \cdot \overline{(\overline{\mathbf{T}^{(\mathbf{n}_k)}}(\mathbf{e}_k) - i\sigma \mathbf{e}_k)}$$
$$- \sum_k \int_{\Gamma_{\boldsymbol{k}}} Q\sigma^{-1} \mathcal{X}_k \cdot \overline{(\overline{\mathbf{T}^{(\mathbf{n}_k)}}(\mathbf{e}_k) - i\sigma \mathbf{e}_k)} = \sum_k \int_{\Gamma_{\boldsymbol{k}}} \sigma^{-1} g \cdot \overline{(\overline{\mathbf{T}^{(\mathbf{n}_k)}}(\mathbf{e}_k) - i\sigma \mathbf{e}_k)} \qquad (51)$$

where $\mathcal{X}_k = \mathbf{T}^{(\mathbf{n}_k)}(\mathbf{u}_k) - i\sigma \mathbf{u}_k$ on $\partial\Omega_k$.

Discretization

The solution of the adjoint Navier equation is separated into three components (Helmholtz decomposition): P-wave, SH-wave and SV-wave. Therefore

$$\mathbf{e}_k = \mathbf{e}_{k,P} + \mathbf{e}_{k,SH} + \mathbf{e}_{k,SV} \tag{52}$$

which satisfy $\nabla \times \mathbf{e}_P = 0$ and $\nabla \cdot \mathbf{e}_{SH} = \nabla \cdot \mathbf{e}_{SV} = 0$.

Similarly, the approximation for $\mathcal{X}_k$ is

$$\mathcal{X}_k \approx \sum_{\ell=1}^{p_P^k} \left[x_{k,\ell}^P \left(-\mathbf{T}^{(\mathbf{n}_k)}(\mathbf{e}_{k,\ell}^P) - i\sigma \mathbf{e}_{k,\ell}^P \right) \right] + \sum_{\ell=1}^{p_S^k} \left[x_{k,\ell}^{SH} \left(-\mathbf{T}^{(\mathbf{n}_k)}(\mathbf{e}_{k,\ell}^{SH}) - i\sigma \mathbf{e}_{k,\ell}^{SH} \right) \right] + \sum_{\ell=1}^{p_S^k} \left[x_{k,\ell}^{SV} \left(-\mathbf{T}^{(\mathbf{n}_k)}(\mathbf{e}_{k,\ell}^{SV}) - i\sigma \mathbf{e}_{k,\ell}^{SV} \right) \right].$$

where

$$\mathbf{e}_{k,\ell}^P = \begin{cases} \mathbf{a}_{k,\ell} \exp(i\overline{\kappa}_P \mathbf{a}_{k,\ell} \cdot \mathbf{x}) & \text{in } \Omega_k \\ 0 & \text{elsewhere} \end{cases}$$

$$\mathbf{e}_{k,\ell}^{SH} = \begin{cases} \mathbf{a}_{k,\ell}^{\perp} \exp(i\overline{\kappa}_{SH} \mathbf{a}_{k,\ell} \cdot \mathbf{x}) & \text{in } \Omega_k \\ 0 & \text{elsewhere} \end{cases}$$

$$\mathbf{e}_{k,\ell}^{SV} = \begin{cases} \mathbf{a}_{k,\ell}^{\perp} \times \mathbf{a}_{k,\ell} \exp(i\overline{\kappa}_{SV} \mathbf{a}_{k,\ell} \cdot \mathbf{x}) & \text{in } \Omega_k \\ 0 & \text{elsewhere} \end{cases}$$

where $\mathbf{a}_{k,\ell}$ is the direction of propagation.

Discrete UWVF

Find $\mathcal{X}_{h,k} \in V_{h,k}$, $k = 1, 2, \ldots, N$ such that

$$\sum_k \int_{\partial\Omega_k} \sigma^{-1} \mathcal{X}_{h,k} \cdot \overline{\mathcal{Y}_{h,k}} - \sum_k \sum_j \int_{\Sigma_{k,j}} \sigma^{-1} \mathcal{X}_{h,j} \cdot \overline{F_k(\mathcal{Y}_{h,k})}$$

$$- \sum_k \int_{\Gamma_k} Q \sigma^{-1} \mathcal{X}_{h,k} \cdot \overline{F_k(\mathcal{Y}_{h,k})} = \sum_k \int_{\Gamma_k} \sigma^{-1} g \cdot \overline{F_k(\mathcal{Y}_{h,k})}$$

for all $\mathcal{Y}_{h,k} \in V_{h,k}$, $k = 1, 2, \ldots, N$ where

$$F_k(\mathcal{Y}_{h,k}) \approx \sum_{\ell=1}^{p_P^k} \left[y_{k,\ell}^P \left(\mathbf{T}^{(\mathbf{n}_k)}(\mathbf{e}_{k,\ell}^P) - i\sigma \mathbf{e}_{k,\ell}^P \right) \right]$$

$$+ \sum_{\ell=1}^{p_S^k} \left[y_{k,\ell}^{SH} \left(\mathbf{T}^{(\mathbf{n}_k)}(\mathbf{e}_{k,\ell}^{SH}) - i\sigma \mathbf{e}_{k,\ell}^{SH} \right) \right]$$

$$+ \sum_{\ell=1}^{p_S^k} \left[y_{k,\ell}^{SV} \left(\mathbf{T}^{(\mathbf{n}_k)}(\mathbf{e}_{k,\ell}^{SV}) - i\sigma \mathbf{e}_{k,\ell}^{SV} \right) \right] . \qquad (53)$$

Matrices

The discrete UWVF can be written in a matrix form as

$$(D - C)X = b \quad \Rightarrow \quad (I - D^{-1}C)X = D^{-1}b \tag{54}$$

Matrices D and C are sparse block matrices. Matrix D is a block diagonal and Hermitian.

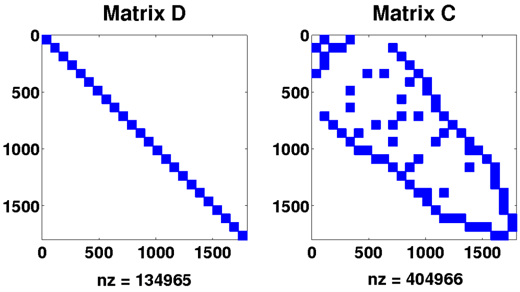

Matrices

A sparse block diagonal matrix is $D = \mathrm{diag}(D^1, D^2, \ldots, D^k, \ldots, D^N)$. One block D^k can be written as

$$D^k = \begin{pmatrix} D^k_{P,P,\ell,m} & D^k_{SH,P,\ell,m} & D^k_{SV,P,\ell,m} \\ D^k_{P,SH,\ell,m} & D^k_{SH,SH,\ell,m} & D^k_{SV,SH,\ell,m} \\ D^k_{P,SV,\ell,m} & D^k_{SH,SV,\ell,m} & D^k_{SV,SV,\ell,m} \end{pmatrix}. \tag{55}$$

where, for example,

$$D^k_{P,SH,\ell,m} = \int_{\partial\Omega_k} \sigma^{-1} \left(-\mathbf{T}^{(\mathbf{n}_k)}(\mathbf{e}^P_{k,m}) - i\sigma\mathbf{e}^P_{k,m}\right) \cdot \overline{\left(-\overline{\mathbf{T}^{(\mathbf{n}_k)}}(\mathbf{e}^{SH}_{k,\ell}) - i\sigma\mathbf{e}^{SH}_{k,\ell}\right)}. \tag{56}$$

Matrices

Sparse matrix C consists of blocks C^k and $C^{k,j}$. Matrix blocks C^k are on the diagonal and $C^{k,j}$ are on the off-diagonal of matrix C. Matrix block C^k can be written as follows

$$C^k = \begin{pmatrix} C^k_{P,P,\ell,m} & C^k_{SH,P,\ell,m} & C^k_{SV,P,\ell,m} \\ C^k_{P,SH,\ell,m} & C^k_{SH,SH,\ell,m} & C^k_{SV,SH,\ell,m} \\ C^k_{P,SV,\ell,m} & C^k_{SH,SV,\ell,m} & C^k_{SV,SV,\ell,m} \end{pmatrix} \tag{57}$$

where, for example, $C^k_{P,SH,\ell,m}$ is of the form

$$C^k_{P,SH,\ell,m} = \int_{\Gamma_k} Q\sigma^{-1} \left(-\mathbf{T}^{(\mathbf{n}_k)}(\mathbf{e}^P_{k,m}) - i\sigma\mathbf{e}^P_{k,m}\right) \cdot \overline{\left(\overline{\mathbf{T}^{(\mathbf{n}_k)}}(\mathbf{e}^{SH}_{k,\ell}) - i\sigma\mathbf{e}^{SH}_{k,\ell}\right)}, \tag{58}$$

similarly others.

Matrices

The off-diagonal block matrix $C^{k,j}$ is as follows

$$C^{k,j} = \begin{pmatrix} C^{k,j}_{P,P,\ell,m} & C^{k,j}_{SH,P,\ell,m} & C^{k,j}_{SV,P,\ell,m} \\ C^{k,j}_{P,SH,\ell,m} & C^{k,j}_{SH,SH,\ell,m} & C^{k,j}_{SV,SH,\ell,m} \\ C^{k,j}_{P,SV,\ell,m} & C^{k,j}_{SH,SV,\ell,m} & C^{k,j}_{SV,SV,\ell,m} \end{pmatrix} \quad (59)$$

where, for example, $C^{k,j}_{P,SH,\ell,m}$ is of the form

$$C^{k,j}_{P,SH,\ell,m} = \int_{\Sigma_{k,j}} \sigma^{-1} \left(\mathbf{T}^{(\mathbf{n}_k)}(\mathbf{e}^{P}_{j,m}) - i\sigma \mathbf{e}^{P}_{j,m} \right) \cdot \overline{\left(\overline{\mathbf{T}^{(\mathbf{n}_k)}}(\mathbf{e}^{SH}_{k,\ell}) - i\sigma \mathbf{e}^{SH}_{k,\ell} \right)}, \quad (60)$$

others can be derived in a similar manner.

Plane wave propagation in a unit cube

The exact solution is of the form

$$\begin{aligned}\mathbf{u} = {} & A_1\mathbf{d}\exp(i\kappa_P\mathbf{x}\cdot\mathbf{d}) + A_2\mathbf{d}_{SH}\exp(i\kappa_S\mathbf{x}\cdot\mathbf{d}) \\ & + A_3\mathbf{d}_{SV}\exp(i\kappa_S\mathbf{x}\cdot\mathbf{d})\end{aligned}$$

where the wave numbers are $\kappa_P = \omega/c_P$, $\kappa_S = \omega/c_S$, the direction $\mathbf{d} \approx [-0.73 \quad 0.45 \quad 0.51]$, $\mathbf{d}_{SH} = \mathbf{d}^{\perp}$, $\mathbf{d}_{SV} = \mathbf{d}^{\perp} \times \mathbf{d}$ and the amplitudes $A_1 = A_2 = A_3 = 1$. In addition, $\nabla \times \mathbf{u}_P = 0$ and $\nabla \cdot \mathbf{u}_{SH} = \nabla \cdot \mathbf{u}_{SV} = 0$. As a boundary condition we choose $Q = 0$.

Flux parameter

In numerical simulations we use an ad hoc choice for coupling parameter (flux parameter) that is

$$\sigma = \omega\rho\mathbb{R}\{c_P\}I \tag{61}$$

where I is the unit matrix.
More investigations of the optimal flux parameter will be investigated in (near) future.

Mesh 1

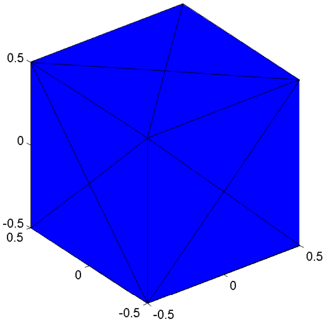

Figure: The mesh. The maximum centroid-vertex distance (element diameter) for element $h = 0.4979$. Number of tetrahedra 24, faces 60 and vertices 14.

Results for p-convergence

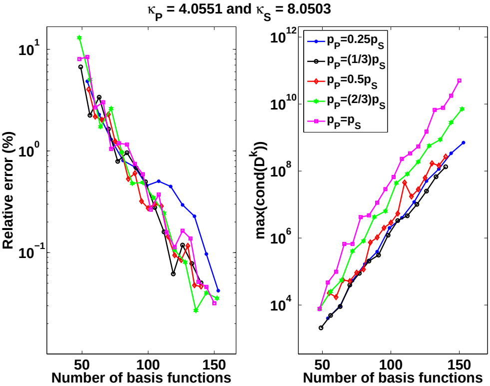

Figure: Results when $\kappa_P = 4.0551$, $\kappa_{SH} = \kappa_{SV} = 8.0503$ with different ratios between p_P/p_S and mesh size is fixed.

Coarsest and densest mesh

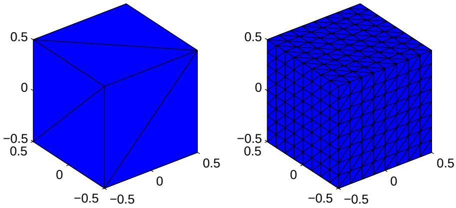

Figure: The coarsest $h_{max} = 0.7395$ and densest meshes $h_{max} = 0.1269$.

Results for h-convergence

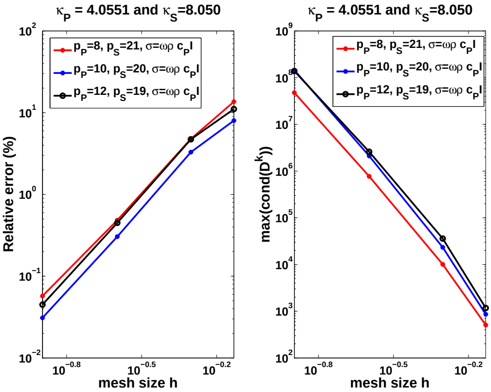

Figure: Results when $\kappa_P = 4.0551$, $\kappa_{SH} = \kappa_{SV} = 8.0503$ with different ratios between p_P/p_S. Number of basis functions per element $p_{tot} = p_P + 2p_S$.

Mesh

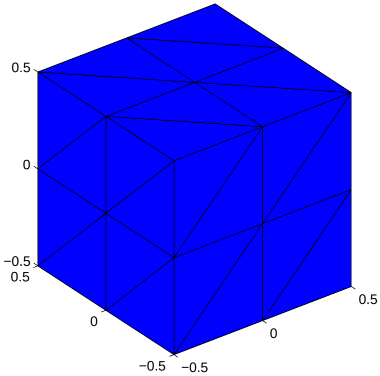

Figure: The mesh when $h_{max} = 0.4978$.

Table: Results when $p_P = 25$ and $p_S = 50$, mesh is fixed and wave number varies.

κ_P	κ_S	error (%)	$\max(\mathrm{cond}(D^k))$
4.0551	8.0503	0.0321	5.8143e8
5.0689	10.0629	0.1319	4.5035e7
6.0826	12.0755	0.4232	5.4503e6
7.0964	14.0881	1.1347	9.2297e5
8.1102	16.1007	1.6142	2.0051e5

FEM, DGM and UWVF

- FEM:
  - uses finite elements such as triangles or tetrahedra
  - uses polynomial test and trial functions (piecewise polynomial)
  - polynomial degree same over the domain

FEM, DGM and UWVF

- FEM:
  - uses finite elements such as triangles or tetrahedra
  - uses polynomial test and trial functions (piecewise polynomial)
  - polynomial degree same over the domain
- standard DGM:
  - uses finite elements such as triangles or tetrahedra
  - uses polynomial test and trial functions (discontinuous)
  - polynomial degrees may vary from element to element
  - allows discontinuities over elements

FEM, DGM and UWVF

- FEM:
  - uses finite elements such as triangles or tetrahedra
  - uses polynomial test and trial functions (piecewise polynomial)
  - polynomial degree same over the domain
- standard DGM:
  - uses finite elements such as triangles or tetrahedra
  - uses polynomial test and trial functions (discontinuous)
  - polynomial degrees may vary from element to element
  - allows discontinuities over elements
- UWVF:
  - uses finite elements such as triangles or tetrahedra
  - uses plane wave test and trial functions (discontinuous)
  - number of basis functions may vary from element to element
  - allows discontinuities over elements

Starting from wave equation

$$\nabla \cdot \left(\frac{1}{\rho} \nabla P(r,t) \right) - \frac{1}{\rho c^2} \frac{\partial^2 P(r,t)}{\partial t^2} = 0, \tag{62}$$

and defining new vectors

$$\boldsymbol{P} = \begin{pmatrix} P_1 \\ P_2 \\ P_3 \\ P_4 \end{pmatrix} = \begin{pmatrix} \frac{\partial P}{\partial t} \\ \frac{1}{\rho} \frac{\partial P}{\partial x_1} \\ \frac{1}{\rho} \frac{\partial P}{\partial x_2} \\ \frac{1}{\rho} \frac{\partial P}{\partial x_3} \end{pmatrix}$$

then we can write the following equations

$$\frac{1}{c^2 \rho} \frac{\partial P_1}{\partial t} - \nabla \cdot \begin{pmatrix} P_2 \\ P_3 \\ P_4 \end{pmatrix} = 0,$$

$$\rho \frac{\partial}{\partial t} \begin{pmatrix} P_2 \\ P_3 \\ P_4 \end{pmatrix} - \nabla \cdot P_1 = 0.$$

References: T. Lähivaara, M. Malinen, J. P. Kaipio, and T. Huttunen, Computational Aspects of the Discontinuous Galerkin Method for the Wave Equation, Journal of Computational Acoustics, Vol. 16, No. 4 (2008) 507-530.
T. Lähivaara and T. Huttunen, A non-uniform basis order for the discontinuous Galerkin method of the 3D dissipative wave equation with perfectly matched layer Journal of Computational Physics, 229(13):5144-5160, 2010
P. Monk and G. R. Richter: A Discontinuous Galerkin Method for Linear Symmetric Hyperbolic Systems in Inhomogeneous Media, Journal of Scientific Computing, Volumes 22 and 23, June 2005, 443- 477

In a matrix form

$$A\frac{\partial P}{\partial t} + \sum_{j=1}^{3} A_j \frac{\partial P}{\partial x_j} = 0 \tag{63}$$

where $A = \mathrm{diag}(\frac{1}{c^2\rho}, \rho, \rho, \rho)$ and

$$A_1 = \begin{pmatrix} 0 & -1 & 0 & 0 \\ -1 & 0 & 0 & 0 \\ 0 & 0 & 0 & 0 \\ 0 & 0 & 0 & 0 \end{pmatrix} \quad A_2 = \begin{pmatrix} 0 & 0 & -1 & 0 \\ 0 & 0 & 0 & 0 \\ -1 & 0 & 0 & 0 \\ 0 & 0 & 0 & 0 \end{pmatrix} \quad A_3 = \begin{pmatrix} 0 & 0 & 0 & -1 \\ 0 & 0 & 0 & 0 \\ 0 & 0 & 0 & 0 \\ -1 & 0 & 0 & 0 \end{pmatrix}$$

References: T. Lähivaara, M. Malinen, J. P. Kaipio, and T. Huttunen, Computational Aspects of the Discontinuous Galerkin Method for the Wave Equation, Journal of Computational Acoustics, Vol. 16, No. 4 (2008) 507-530.
T. Lähivaara and T. Huttunen, A non-uniform basis order for the discontinuous Galerkin method of the 3D dissipative wave equation with perfectly matched layer Journal of Computational Physics, 229(13):5144-5160, 2010
P. Monk and G. R. Richter: A Discontinuous Galerkin Method for Linear Symmetric Hyperbolic Systems in Inhomogeneous Media, Journal of Scientific Computing, Volumes 22 and 23, June 2005, 443- 477

Weak form in DGM is

$$\int_{\Omega_{\boldsymbol{k}}} \boldsymbol{v}^T \left(A \frac{\boldsymbol{P}}{\partial t} + \sum_{j=1}^{3} A_j \frac{\partial \boldsymbol{P}}{\partial x_j} \right) \tag{64}$$

$$= \int_{\Omega_{\boldsymbol{k}}} \boldsymbol{v}^T A \frac{\partial \boldsymbol{P}}{\partial t} - \sum_{j=1}^{3} \frac{\partial \boldsymbol{v}^T}{\partial x_j} A_j \boldsymbol{P} + \int_{\Gamma(\Omega_{\boldsymbol{k}})} \boldsymbol{v}^T \mathcal{F} \boldsymbol{P} = 0 \tag{65}$$

where $\mathcal{F}$ is the flux matrix. On the other hand $\mathcal{F} = \mathcal{F}^+ + \mathcal{F}^-$ where

$$\mathcal{F}^+ = \frac{1}{2} \begin{pmatrix} -1 \\ n_1 \\ n_2 \\ n_3 \end{pmatrix} (-1, n_1, n_2, n_3), \quad \mathcal{F}^- = -\frac{1}{2} \begin{pmatrix} 1 \\ n_1 \\ n_2 \\ n_3 \end{pmatrix} (1, n_1, n_2, n_3)$$

References: T. Lähivaara, M. Malinen, J. P. Kaipio, and T. Huttunen, Computational Aspects of the Discontinuous Galerkin Method for the Wave Equation, Journal of Computational Acoustics, Vol. 16, No. 4 (2008) 507-530.
T. Lähivaara and T. Huttunen, A non-uniform basis order for the discontinuous Galerkin method of the 3D dissipative wave equation with perfectly matched layer Journal of Computational Physics, 229(13):5144-5160, 2010
P. Monk and G. R. Richter: A Discontinuous Galerkin Method for Linear Symmetric Hyperbolic Systems in Inhomogeneous Media, Journal of Scientific Computing, Volumes 22 and 23, June 2005, 443- 477

Finally we can write

$$\int_{\Omega_k} \boldsymbol{v}^T \left(A \frac{\boldsymbol{P}}{\partial t} + \sum_{j=1}^{3} A_j \frac{\partial \boldsymbol{P}}{\partial x_j} \right) + \int_{\Gamma_i(\Omega_k)} \boldsymbol{v}^T \mathcal{F}^- (\tilde{\boldsymbol{P}} - \boldsymbol{P}) \tag{66}$$

$$- \int_{\Gamma_e(\Omega_k)} \boldsymbol{v}^T (\mathcal{F} - \mathcal{N}) \boldsymbol{P} + \int_{\Gamma_e(\Omega_k)} \boldsymbol{v}^T \boldsymbol{g} \tag{67}$$

where we have used the knowledge that $\mathcal{F}^- \tilde{\boldsymbol{P}} = \mathcal{F}^- \boldsymbol{P}$ and $(\mathcal{F} - \mathcal{N})\boldsymbol{P} = \boldsymbol{g}$.

References: T. Lähivaara, M. Malinen, J. P. Kaipio, and T. Huttunen, Computational Aspects of the Discontinuous Galerkin Method for the Wave Equation, Journal of Computational Acoustics, Vol. 16, No. 4 (2008) 507Ű530.

T. Lähivaara and T. Huttunen, A non-uniform basis order for the discontinuous Galerkin method of the 3D dissipative wave equation with perfectly matched layer Journal of Computational Physics, 229(13):5144-5160, 2010

P. Monk and G. R. Richter: A Discontinuous Galerkin Method for Linear Symmetric Hyperbolic Systems in Inhomogeneous Media, Journal of Scientific Computing, Volumes 22 and 23, June 2005, 443- 477

Summary of the UWVF and DGM

- Above wave equation based weak formulation can be modified into the time-harmonic equation
- The UWVF is an upwind discontinuous Galerkin method
- Differences between the UWVF and standard DGM are the form of the fluxes, basis functions and degrees of freedom
- Fluxes and averages over the elements play important role in the derivation of variational formulations
- Discontinuities allowed in the basis functions

- Bérenger J. A perfectly matched layer for the absorption of electromagnetic waves. Journal of Computational Physics 114:185-200,1994.
- Cessenat O. Application d'une nouvelle formulation variationnelle aux équations d'ondes harmoniques. Probl'emes de Helmholtz 2D et de Maxwell 3D., PhD thesis. Université Paris IX Dauphine, 1996.
- Cessenat O, Després B. Application of an ultra weak variational formulation of elliptic PDEs to the two-dimensional Helmholtz problem. SIAM Journal on Numerical Analysis 35(1):255–299, 1998.

Finnish Centre of Excellence in Inverse Problems Research
UNIVERSITY OF EASTERN FINLAND

Cessenat O, Després B. Using plane waves as base functions for solving time harmonic equations with the ultra weak variational formulation. Journal of Computational Acoustics, 11(2):227–238,2003.

Huttunen T The ultra weak variational formulation for ultrasound transmission problems. PhD-thesis, 2004.

Huttunen T, Monk P, Kaipio JP. Computational aspects of the ultra-weak variational formulation. Journal of Computational Physics, 182(1):27–46,2002.

Huttunen T, Monk P, Collino F, Kaipio JP. The ultra weak variational formulation for elastic wave problems. SIAM Journal on Scientific Computing, 25(5):1717–1742, 2004.

- Huttunen T, Kaipio JP., Monk P. The perfectly matched layer for the ultra weak variational formulation of the 3D Helmholtz equation. International Journal for Numerical Methods in Engineering 61(7): 1072 –1092, 2004.
- Huttunen T, Seppälä ET, Kirkeby O, Kärkkäinen A, Kärkkäinen L. Simulation of the transfer function for a head-and-torso model over the entire audible frequency range. Journal of Computational Acoustics, 15(4):429–448, 2007.
- Luostari T, Huttunen T, Monk P. The ultra weak variational formulation using Bessel basis functions, Communications in Computational Physics (Special issue of Waves 2009 conference), (In press).

- Lähivaara T, Malinen M, Kaipio JP, Huttunen T. Computational Aspects of the Discontinuous Galerkin Method for the Wave Equation. Journal of Computational Acoustics, 16 (4):507–530, 2008.
- Lähivaara T, Huttunen T. A non-uniform basis order for the discontinuous Galerkin method of the 3D dissipative wave equation with perfectly matched layer. Journal of Computational Physics, 229(13):5144-5160, 2010
- Monk P, Richter G. R. A Discontinuous Galerkin Method for Linear Symmetric Hyperbolic Systems in Inhomogeneous Media. Journal of Scientific Computing, 22-23, 443–477, 2005

- Brenner SC., Scott LR. The mathematical theory of finite element methods Springer, 1994.
- Ihlengburg F. Finite element analysis of Acoustic Scattering. Springer, 1998.
- Kinsler L.E, Frey A.R, Coppens A.B, Sanders J.V. Fundamentals of Acoustics. Wiley; (4 edition (December 30, 1999))
- Monk P. Finite Element Methods for Maxwell's Equations. Oxford University Press, USA, 2003.

Acknowledgements

Authors thank from the support

- Finnish Graduate School in Computational Sciences (FICS)
- Finnish Centre of Excellence in Inverse Problems Research